PROCEEDINGS OF SCIENCE

Prospects for Gamma Ray Bursts detection with LHAASO

S.Z. Chen,[a] T. Di Girolamo,[b,c] H.H. He,[a] P. Vallania,[d,e] C. Vigorito*,[e,f] H.R. Wu,[a] Z.G. Yao[a] and F.R. Zhu[g] for the LHAASO Collaboration†

[a] *Key Laboratory of Particle Astrophysics, Institute of High Energy Physics, Chinese Academy of Science, P.O. Box 918, 100049 Beijing, Republic of China*

[b] *Dipartimento di Fisica dell'Università di Napoli "Federico II", Complesso Universitario di Monte Sant'Angelo, via Cinthia, I-80126 Napoli, Italy*

[c] *Istituto Nazionale di Fisica Nucleare, Sezione di Napoli, Complesso Universitario di Monte Sant'Angelo, via Cinthia, I-80126 Napoli, Italy*

[d] *Osservatorio Astrofisico di Torino dell'Istituto Nazionale di Astrofisica, via P. Giuria 1, I-10125 Torino, Italy*

[e] *Istituto Nazionale di Fisica Nucleare, Sezione di Torino, via P. Giuria 1, I-10125 Torino, Italy*

[f] *Dipartimento di Fisica dell'Università di Torino, via P. Giuria 1, I-10125 Torino, Italy*

E-mail: vigorito@to.infn.it

[g] *Southwest Jiaotong University, 610031 Chengdu, Sichuan, Republic of China*

The LHAASO (Large High Altitude Air Shower Observatory) experiment, currently under design, is planned to be installed in the Sichuan Province (China) at 4410 m a.s.l. with the aim of studying the highest energy gamma-ray sources and cosmic rays in the wide energy range from hundreds of GeV to hundreds of TeV. Among its different components, optimized to study different energy regions, the WCDA (Water Cherenkov Detector Array) will be one of the most important. Four ponds, 150x150 m^2 each, will be equipped with 3600 PMTs to detect the Cherenkov light produced by ultra-relativistic particles. Each PMT will monitor a volume cell of 5x5x4 m^3. Data (signal amplitude, with a threshold set at 1 pe level, and arrival time) from each PMT are collected and sent to a DAQ system able to build and record events with all multiplicities starting from a single PMT fired. For small numbers, the primary energy for gammas corresponds to a few GeV, well overlapping the actual satellite detectors. In this paper, the scheme to calculate the expected rate and typology of GRBs detectable in follow-up mode with LHAASO is described and discussed.

The 34th International Cosmic Ray Conference,
30 July- 6 August, 2015
The Hague, The Netherlands

*Speaker.

†This work is supported in China by NSFC (grants 11205165, 11375210, 11375224, 11405181, 11475190), the Chinese Academy of Science, Institute of High Energy Physics, the Key Laboratory of Particle Astrophysics, CAS and in Italy by the Istituto Nazionale di Fisica Nucleare (INFN).

PoS(ICRC2015)728

1. Introduction

Gamma Ray Bursts are among the most powerful sources in the sky, with an energy spectrum extending from radio to gamma rays of tens of GeV. They occur with a frequency of a few per day, and originate from the entire universe.

GRBs are divided into two classes depending on their duration. The short ones last up to 2 seconds and show a harder spectrum with a mean peak energy of 490 keV. It is believed that their origin is due to the merger of two compact objects such as neutron stars or blacks holes. Long GRBs have durations greater than 2 seconds with a softer spectrum and a peak at about 160 keV. In this case it is thought that the origin is due to the collapse of the nucleus of a type Ib/c Supernova, and in fact, the coincidence between these two phenomena has already been observed in many cases. The shape of the spectrum is well described in most cases by the Band function, characterized by two power laws smoothly connected. Although the majority of the ejection is concentrated in the energy region between keV and MeV, some photons have been observed up to tens of GeV using detectors in space on board the CGRO satellite and more recently Fermi and AGILE.

Until now all the experimental data in the MeV - GeV energy range were obtained from detectors onboard satellites, but due to their small size and the rapid fall of GRB energy spectra they hardly cover the energy region above 1 GeV. The detection on ground can be done by two kinds of detectors able to provide a much larger effective area: telescopes for the atmospheric Cherenkov light and EAS arrays.

With their enormous size, the Cherenkov telescope recently installed at HESS and those planned for the CTA observatory allow the detection of gamma rays with an energy threshold as low as 20 GeV. However, the necessity of working during nights with clear skies and no or few moon light limits the efficiency to 10-15 %. Furthermore, apart very seldom serendipitous observations or specific pointing strategies to cover a wider sky region, the field of view of less than about 5° prevents the study of short GRBs and of the prompt phase of long GRBs, since the repointing requires a minimum time of about 100 seconds. So far, all major Cherenkov detectors (MAGIC, HESS, VERITAS) have tried to point the GRBs following the afterglow but without success. In the case of CTA it is expected a coincident detection of 0.5 - 2 GRBs per year [3] depending on the assumed high energy spectral features, satellite alert rate and array performance.

The EAS arrays have on the contrary a large field of view (nominally 2 sr, limited only by the atmospheric absorption) and high efficiency (up to 100%), but the need to reveal enough secondary particles to reconstruct the arrival direction and energy of the primary increases the threshold to around 100 GeV.

An alternative mode consists in the measurement of the counting rates of the detectors at time intervals of the order of a fraction of second ("single particle technique") [4, 5, 6], and then in the search for an excess in coincidence with a GRB detected by a satellite. With this technique it is not possible to measure the arrival direction of the excess, but the threshold energy can be lowered to about 1 GeV. Both techniques have been used by various extensive air shower arrays, such as EASTOP, Chacaltaya, Milagro and more recently ARGO-YBJ which has studied the richest sample of GRBs ever analyzed by a detector on ground (over 200 events) [7]. Even in this case there has been no clear detection.

The HAWC experiment, an extensive air shower array with an area of 22,000 m^2 fully operat-

ing in Mexico since spring 2015 at an altitude of 4100 m a. s. l., has made a detailed study on the possibility of detecting GRBs with both techniques, estimating an overall detection rate of 1.55/y for short GRBs and 0.25/y for long ones [8, 9]. The shower technique was found to be preferred with the idea of lowering the threshold energy down to 50 GeV. In this paper a method similar to that used for CTA and HAWC to calculate the expected rate and features of detectable GRBs has been applied to LHAASO.

2. The LHAASO experiment

The LHAASO experiment, planned to be installed in the Sichuan Province (P.R. of China) at 4410 m a.s.l., is currently under design to study cosmic rays and photons in the energy range 0.1 - 1000 TeV. This very wide interval is obtained combining different air shower detection techniques covering different energy windows. At the lower end, from 100 GeV to 30 TeV, the Water Cherenkov Detector Array (WCDA) is one of the major components of LHAASO. It is made of four ponds, 150 $\times$ 150 m^2 each, covering a total surface of 90000 m^2. Each pond is divided into 900 cells (5 $\times$ 5 m^2 each, with a depth of 4 m) seen by one PMT located at the cell floor centre and looking up to detect the direct Cherenkov light produced by the relativistic particles of the showers. In order to maximize the detector performance a large simulation campaign has been carried out to optimize both the cell dimensions and depth and the number of PMTs for each cell. The results show that a higher PMT density, obtained with both smaller cells and higher number of PMTs per cell gives a better performance in terms of angular resolution and sensitivity, but weighting these results with a cost estimate the 5 $\times$ 5 m^2 cells seen by a unique PMT offer the most effective layout [10]. Besides simulations, a prototype water Cherenkov detector has been built and operated in Beijing and an engineering array corresponding to 1% of one pool (3 $\times$ 3 cells equipped with one 8" Hamamatsu R5912 PMT each) has been implemented at the ARGO-YBJ site (Yangbajing Cosmic Ray Laboratory, 4300 m a.s.l., P.R. of China). The measured counting rate was about 35 kHz for each cell, with an expected minimum of 12.5 kHz given by cosmic rays. Since LHAASO will be located at a similar height, we foresee a counting rate close to this value. This very high single counting rate does not allow a simple majority but requires a topological one, with different trigger levels. The basic element is given by a 3 $\times$ 3 cells matrix, whose signal is collected by a custom FEE and sent to a station where a suitable trigger is generated and the corresponding data are recorded. This quite new approach is called "triggerless" and allows the maximum DAQ flexibility. For example, overlapping the clusters (corresponding to 12 $\times$ 12 cells) by shifting them of 30 m and requiring a coincidence of at least 12 PMTs within 250 ns in any cluster, a trigger rate of 70 KHz is expected. In the search for GRBs, this approach is particularly effective. For very low multiplicities, starting from 3, the number of random coincidences does not allow the reconstruction of the arrival direction, and moreover the huge amount of events prevents the storage of data. However, if an on-line alert is provided by satellites, as for the case of Cherenkov telescopes, the DAQ can switch to this very low multiplicity mode for a limited amount of time ($\sim$ minutes) and knowing the arrival direction the random coincidences can be strongly suppressed. Even if for these very low multiplicity events ($\sim$ 3-10 hits) the angular resolution is very poor ($\sim$ 10-15°) and the primary energy is very badly reconstructed, the background is highly reduced with respect to the single particle technique, where the contribution comes from the whole sky. Providing a buffer

to store continuously some tens of seconds of low multiplicity data, the GRBs can be followed since the beginning covering the delay of the alert transmission. More details and first estimates of the sensitivity achievable with this technique are given in the paper "Low multiplicity technique for GRB observation by LHAASO-WCDA" by H.R. Wu, H.H. He et al., these proceedings. To sum up, the GRB search will be done by LHAASO using the WCDA data in three different ways, depending on multiplicity:

- for n=1,2 or slightly higher number of particles, the DAQ will simply count the number of events in a fixed time window with the corresponding multiplicity and the search will be done in "scaler mode", looking for a statistical excess in the counting rate of all the PMTs in the detector;
- for n$\gtrsim$10 the events are reconstructed one by one and an excess is looked for in the GRB direction. Since all these data are recorded, this search can be done off-line with unlimited GRB duration;
- for the intermediate multiplicities, data are recorded for a fixed time window before and after the real-time alert given by satellites. If successful, this technique will cover for the first time for EAS arrays the energy region between a few GeV and 100 GeV with some directional information.

In order to evaluate the rate and typology of GRBs detectable by LHAASO, several ingredients must be laid together and precisely a GRB model, a parametrization as a function of energy of the detector performance (effective area and angular resolution) and some hypotheses on the expected external trigger rate. All these items will be presented and discussed in the following sections.

3. The GRB model

To compare our results with CTA and mainly HAWC, we decided to use the same approach found in [11] and [12]. In these papers, a set of pseudo-GRBs has been simulated sampling their features from the experimental ones measured by Fermi (GBM and LAT) and Swift (BAT) satellites. At first, we assume that the external trigger will be given by Fermi-GBM. For each parameter, a different distribution has been considered for short ($T_{90} \leq 2$ s) and long ($T_{90} > 2$ s) GRBs, and no correlation among them has been considered.

3.1 The high energy spectrum

We suppose a high energy emission in the 1-1000 GeV energy range as a simple power law with fixed spectral index and no intrinsic cutoff, that will be given exclusively by Extragalactic Background Light (EBL) absorption. To quantify this high energy contribution, we used the correlation between the fluences measured by GBM and LAT, respectively in the low and high energy bands. Fig. 1 shows this correlation, updated with all the 21 GRBs with fluence calculated in the same time window. The points are very scattered, and for short GRBs (red squares) only 3 events were measured by both detectors. Nevertheless we followed the assumptions made in [13] that the LAT fluence in the 100 MeV-10 GeV energy range is about 10% of the GBM fluence in the 10 keV-1 MeV energy range for long GRBs, while for short ones the amount is 100%.

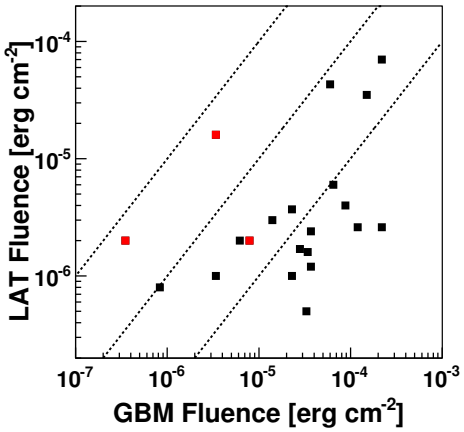

Figure 1: A comparison of the LAT and GBM fluences in the [0.1-10] GeV and [10-1000] MeV range respectively. Black (red) squares are for long (short) GRBs; dashed lines indicate LAT-GBM fluence ratio of 0.1, 1.0, 10.0 (bottom to top).

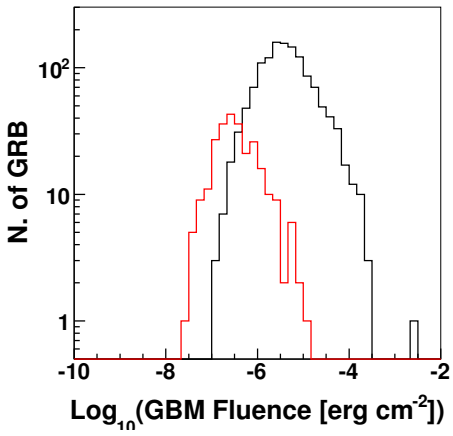

Figure 2: Distribution of measured GBM fluences for Long (black) and Short (red) GRBs in the [10-1000] MeV range.

Fig. 2 shows the low energy fluence measured by GBM (red: short GRBs; black: long GRBs). For the high energy emission of our pseudo-GRBs we sampled from these distributions a fluence that is reported to the 100 MeV-10 GeV energy region using the quoted percentages. Since the fluence distribution for long GRBs is shifted towards larger values by about a factor of 10 with respect to the short ones, the high energy scaling produces a close distribution for short and long GRBs. For the high energy spectrum we used a spectral index α = -2, since for long GRBs with an additional power law this is the mean value measured by LAT. For short GRBs we used α = -1.6, the same value used in [12]. The assumption that all short and long GRBs have an additional high energy power law with spectral index -1.6 and -2, respectively, and without any cutoff in all the considered energy range is quite raw and optimistic, but in any case it allows us to compare our results with the expected sensitivity of HAWC.

3.2 The light curve

As pointed out by Ghisellini et al. in [14], the GRB light curve can be modelled as a constant flux during the T_{90} measured by GBM, followed by a power law fall-off with index γ=1.5. Due to its expected higher sensitivity and to the fact that it will lose the prompt phase of most GRBs, CTA made this assumption in [11] to estimate the rate of detectable GRBs. We decided instead to follow the approach used for HAWC, i.e., we sampled the T_{90} distribution showed in Fig. 3 obtained by Fermi-GBM for long GRBs (black line), while we used a fixed GRB duration of 2 s for short GRBs.

3.3 The EBL absorption

The interaction of very high energy photons with the EBL produces e-pairs and thus a quite sharp spectral cutoff. This absorption depends on the redshift and GRBs are cosmological objects, with a mean value $z \simeq 2$. Many models of EBL attenuation have been published in the last decades, with a general trend towards an increase of transparency due to the observation of very high energy

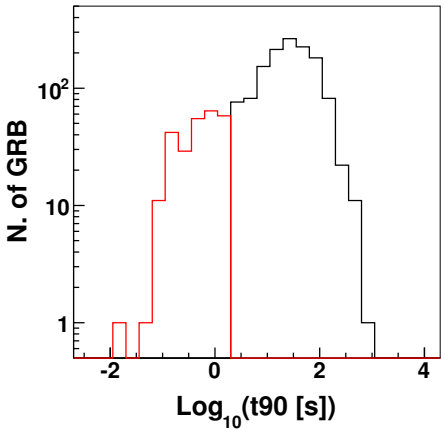

Figure 3: Distribution of T_{90} durations for Long (black) and Short (red) GRBs detected by Fermi-GBM.

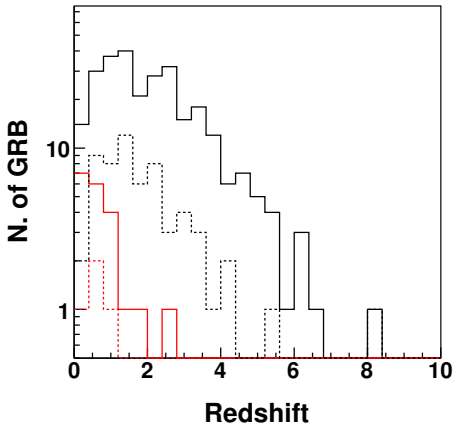

Figure 4: Distribution of redshift for Long (black) and Short (red) GRBs detected by Fermi-GBM. Dashed lines show the subsamples of Long and Short GRBs observed simultaneously by Fermi-GBM and Swift-BAT detectors.

photons at larger redshifts [15]. In this work we used the model by Kneiske et al. [16]. Since the energy resolution of the Fermi-GBM instrument does not allow the detection of clear spectral lines, the GRB distance is obtained sampling the redshift distributions measured by Swift-BAT. Fig. 4 shows these distributions for long (black line) and short (red line) GRBs. We apply the EBL cutoff starting from z=0.1 and up to 1 TeV, the maximum energy after which the source spectrum is totally absorbed. This choice is due to the fact that z=0.1 corresponds roughly to a cutoff energy of 1 TeV in our model. An important point to be checked is that the higher sensitivity of Swift-BAT with respect to Fermi-GBM could distort the redshift distribution, so we selected the subsample of GRBs detected by both. The corresponding distribution (dashed black and red lines for long and short GRBs respectively) is also shown in Fig. 4 and does not show significant deviations from the whole data set.

4. The detector performance for the different configurations

The sensitivity of an EAS array to any gamma-ray source and in particular to GRBs is given by the angular resolution and the effective area for primary photons. Both of these depend on the primary energy and on the zenith angle (however, the dependency of the angular resolution on the zenith angle is small). The expected performance of the detector is evaluated by means of a detailed Monte Carlo simulation that reproduces the development of gamma-ray showers in the atmosphere and the interaction of the secondary EAS particles with the detector. For each pseudo-GRB the expected signal S is calculated integrating from 1 GeV to 1 TeV:

$$S = \int_{1\ GeV}^{1\ TeV} S_\gamma(E) \times EBL(E,z) \times A^\gamma_{eff}(E,\theta) \times T_{90}\ dE \tag{4.1}$$

where $S_\gamma(E)$ is the sampled GRB spectrum, $EBL(E,z)$ the EBL absorption, $A^\gamma_{eff}(E,\theta)$ the photons effective area and T_{90} the burst duration. The peak energy E_{peak} is defined as the energy corresponding to the maximum of the signal function before integration. For GRBs, E_{peak} is tipically less than 100 GeV.

The zenith angle of the pseudo-GRB is randomly chosen in the range from 0 to 50 degrees, with a uniform distribution in the corresponding solid angle. To calculate the expected background B, the same Monte Carlo simulation is run for primary protons, obtaining an effective area $A^p_{eff}(E,\theta)$ as a function of energy and zenith angle. The expected background B is calculated integrating in the same energy range 1GeV-1 TeV:

$$B = \int_{1\ GeV}^{1\ TeV} S_p(E) \times A^p_{eff}(E,\theta) \times T_{90} \times \Omega(E_{peak})\ dE \tag{4.2}$$

where $S_p(E)$ is the cosmic ray spectrum and $\Omega(E_{peak})$ the solid angle corresponding to the angular resolution for $E = E_{peak}$. As angular resolution, we use the Ψ_{70} aperture that maximizes the signal to noise ratio keeping 71.5% of the signal with an aperture of 1.58 σ.

For the cosmic ray spectrum, an accurate simulation of all the primary nuclei from p to Fe should be made and the corresponding effective areas obtained, but an usual short cut foresees to consider a cosmic ray flux made only by protons. For each primary particle (in our case photons and protons) this simulation procedure, that is very CPU-consuming requiring the generation of a huge amount of events, must be repeated for each trigger condition and several zenith angles. Fig. 5 shows the angular resolution for a trigger multiplicity n $\geq$ 20 while Fig. 6 shows the corresponding effective areas for gamma rays (black dots) and protons (red dots) with zenith angle in the [10-30]° range. These results have been obtained using CORSIKA [17] for the development of EASs from gamma rays and protons, and a custom software derived by the Milagro one for the detector response. The complete set of simulations for the different trigger conditions is currently undergoing.

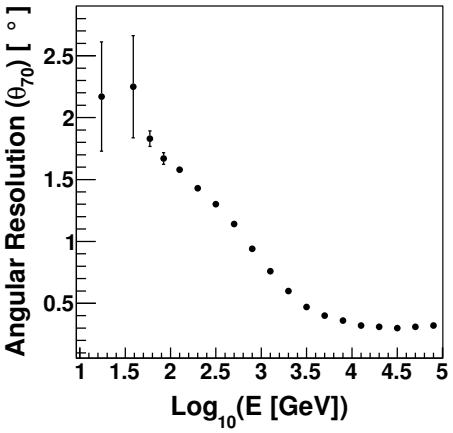

Figure 5: Expected angular resolution of the WCDA.

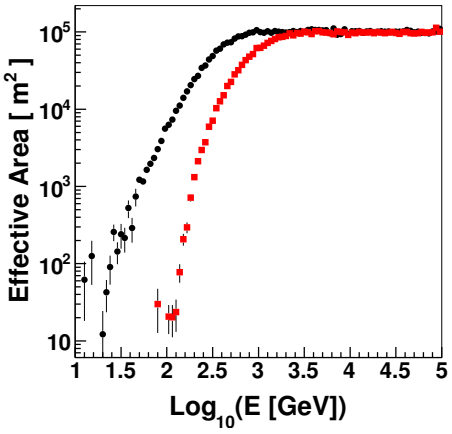

Figure 6: Effective areas for gamma rays (black dots) and protons (red squares) of the WCDA.

5. The detector threshold and external trigger rate

The confidence level of a detection is obtained requiring a signal greater than a given number of background fluctuations. A value of 5 s.d. has been set as the detector threshold, and to properly calculate the signal significance we used equation (17) of [18]. Once the fraction of detectable GRBs has been derived, an external trigger rate must be provided. According to [19], Fermi/GBM detected GRBs with a mean detection rate of $\sim$ 250 yr^{-1} in its f.o.v. of 8.74 sr. This corresponds

to more than 700 GRBs yr^{-1} from the whole sky taking into account that GBM has a duty cycle of about 50%. The LHAASO angular acceptance up to 50° in zenith angle is 2.24 sr, with a full sky coverage of 17.9%. The expected trigger rate in GBM follow-up observations is thus 45 yr^{-1}, while in independent mode we foresee $\sim$ 130 "GBM-like" GRBs per year. These values will be used to normalize in time our pseudo-GRBs data set.

6. Discussion and conclusions

CGRO/EGRET in the past and recently Fermi/LAT have clearly demonstrated the emission of GeV photons from GRBs. Nevertheless, this VHE emission is quite unusual and the presence of a hard power-law contribution to the spectrum has not been confirmed for all the GRBs seen by LAT. Moreover, the extrapolation to the GeV region is made over several orders of magnitude, with a fixed ratio between low and high energy fluences that roughly fits reality. The expected fraction of detectable GRBs is largely dependent on the adopted GRB model, and for this reason we decided to use as much as possible the same assumptions made by CTA and mainly by HAWC to make the results comparable. Presently, our GRB model is defined together with all the calculation details. The determination of the effective area and angular resolution for gamma rays and protons and for the different trigger conditions is currently under way and the very first results on the GRBs detectability and typology for some trigger conditions by LHAASO-WCDA are under check. During the Conference we will possibly show preliminary estimates.

References

[1] B. Zhang, *Int. J. of Mod. Phys. D*, **23**, 1430002 (2014).

[2] P. Mészáros and M.J. Rees, arXiv:1401.3012 (2014).

[3] R.C. Gilmore et al., *Exp. Astron.* **35**, 413 (2013).

[4] S. Vernetto, *Astropart. Phys.* **13**, 75 (2005).

[5] G. Aielli et al., *Astropart. Phys.* **30**, 85 (2008).

[6] G. Aielli et al., *Astrophys. J.* **699**, 1281 (2009).

[7] B. Bartoli et al., *Astrophys. J.* **794**, 82 (2014).

[8] A.U. Abeysekara et al., *Astropart. Phys.* **35**, 641 (2012).

[9] A. Tepe et al., *Adv. Sp. Res.* **49**, 103 (2012).

[10] Li Hui-Cai et al., *Chinese Physics C* **38**, 1 (2014)

[11] R.C. Gilmore et al., *Exp. Astronom.* **35**, 413 (2013).

[12] I. Taboada & R.C. Gilmore, *Nucl.Instrum.Meth. A* **742**, 276 (2014).

[13] M. Ackermann et al., *ApJS* **209**, 11 (2013).

[14] G. Ghisellini et al., *MNRAS* **403**, 926 (2010).

[15] G.I. Rubtsov & S.V. Troitsky, *JETP Letters* **100**, 355 (2014).

[16] T.M. Kneiske et al., *A&A* **413**, 807 (2004).

[17] D. Heck et al., *Report No. FZKA 6019, Forschungszentrum Karlsruhe* (1998).

[18] T. Li & Y. Ma, *ApJ* **272**, 317 (1983).

[19] A. von Kienlin et al., *ApJS* **211**, 13V (2014).